



Pd-porphyrin functionalized ionic liquid-modified mesoporous SBA-15: An efficient and recyclable catalyst for solvent-free Heck reaction

Jing Zhang^a, Guo-Feng Zhao^a, Zora Popović^b, Yong Lu^a, Ye Liu^{a,*}

^a Shanghai Key Laboratory of Green Chemistry and Chemical Processes, Chemistry Department, East China Normal University, Shanghai 200062, China

^b General and Inorganic Laboratory, Chemistry Department, University of Zagreb, HR-10000 Zagreb, Croatia

ARTICLE INFO

Article history:

Received 2 February 2010

Received in revised form 29 June 2010

Accepted 16 July 2010

Available online 23 July 2010

Keywords:

- A. Composites
- A. Organic compounds
- B. Chemical synthesis
- D. Catalytic properties

ABSTRACT

The Pd-porphyrin functionalized ionic liquid could be covalently anchored in the channels of mesoporous SBA-15 through ion-pair electrostatic interaction between imidazolium-cationic and Pd-porphyrin-anionic moieties. Such modified SBA-15 materials were prepared successfully via a post-synthesis (surface sol-gel polymerization) or a one-pot sol-gel procedure, which were characterized by powder X-ray diffraction, UV-visible spectroscopy, Fourier transform infrared spectroscopy, N₂ sorption, elemental analysis, and transmission electron microscopy. The modified SBA-15 materials are efficient and recyclable catalysts for cross-coupling of aryl iodides or activated aryl bromides with ethyl acrylate without activity loss and Pd leaching even after 9 runs.

© 2010 Elsevier Ltd. All rights reserved.

1. Introduction

The palladium catalyzed Heck reaction is one of the most widely used catalytic carbon-carbon bond forming tools in organic synthesis to achieve substituted alkenes, dienes, and other unsaturated structures, many of which are important intermediates in the natural product synthesis and in the production of fine chemicals [1]. For a great variety of Pd-catalysts applied in homogenous processes, Heck reaction suffers from disadvantages like large amount of volatile solvents required, toxic and air/moisture phosphine ligands used, Pd-catalyst recovery and recyclability unavailable [1,2]. Thus, the immobilization of palladium catalyst on a solid support like polymer, inorganic oxides, zeolites, etc. has attracted considerable attention [3–7]. However, organic synthesis using supported insoluble catalysts leads to a series of problems including mass transfer limitation, decreased activity, catalysts leaching out of the solid support, etc. This has led to alternative “liquid phase” methodologies with the aim to “restore” homogeneous reaction conditions, like using ionic liquids (ILs) as mobile and versatile “carriers” [8–13], “soluble polymer supports” [14,15], and “fluorous phase” [16,17].

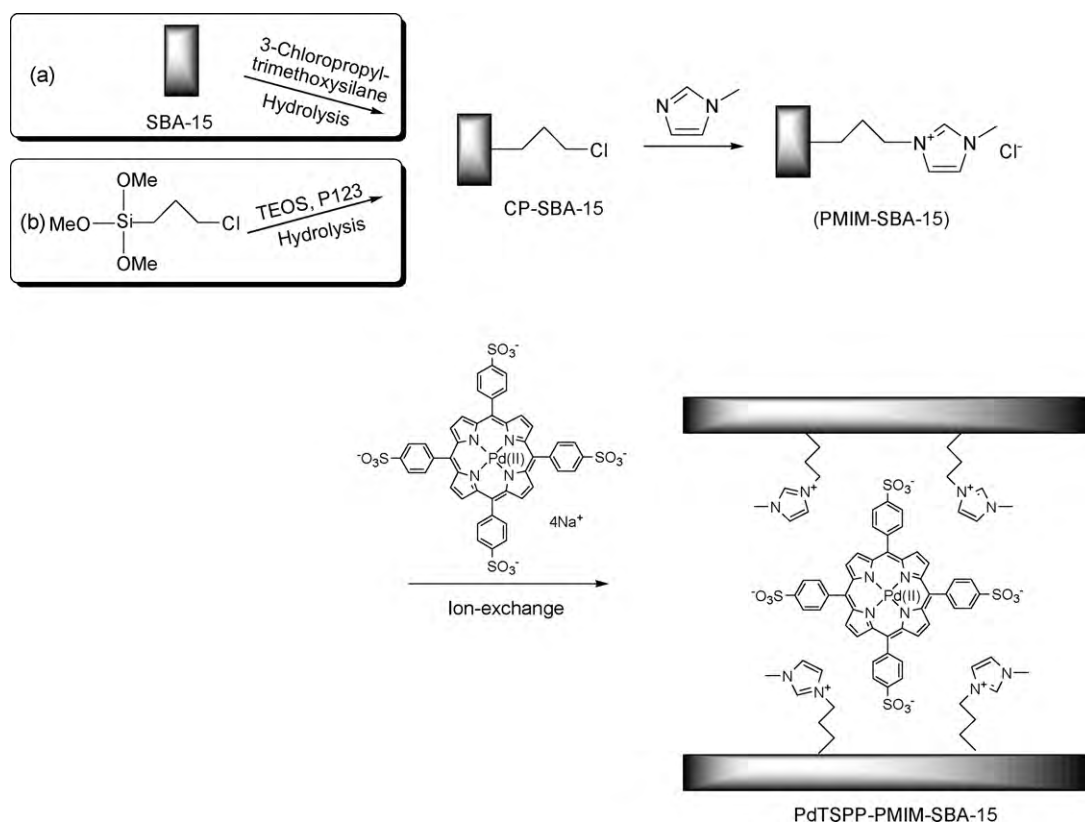
More recently, the supported-IL-phase (SILP) catalysis [18–20] has been shown as an alternative approach for the development of novel heterogeneous catalysts with advantages of facilitating separation workup and “restoring” homogeneous catalytic efficien-

cy [21–26]. Another advantage of supported-IL phases over IL-liquid phases is in minimizing the amounts of costly ILs which may affect the economic viability of a potential process when environmentally benign syntheses are being considered [27,28]. In numerous solid supports applied in SILP catalysis, mesoporous silica, such as SBA-15 [29] and MCM-41 [30], with good thermal/oxidative stability, highly ordered channel structures of pore diameter in the range of 1.5–30 nm, and huge internal surface areas of 700–1000 m²/g [31], are suitable supports to accommodate functionalized ILs (as catalysts) and facilitate the diffusion of bulky reactant molecules.

In this work, the Pd-porphyrin functionalized IL was covalently anchored in the channels of mesoporous SBA-15 via ion-pair electrostatic interaction, aiming to develop a new heterogeneous catalyst for the Heck reaction of aryl iodides (or aryl bromides) and ethyl acrylate without defeating the activity of Pd-porphyrin catalyst and forfeiting the nature of heterogeneous catalysis. Scheme 1 shows the strategy for synthesizing the SBA-15 supported anionic (meso-tetra-(p-sulfonatophenyl)-porphyrinato)palladium ([PdTSPP]⁴⁻) catalyst, which is confined in the channels of imidazolium-based IL-modified SBA-15 (PMIM-SBA-15) tightly and stoichiometrically through electrostatic interaction. The imidazolium cations which are covalently and stoichiometrically bonded to SBA-15 act as the linkers between SBA-15 and the catalytic sites of [PdTSPP]⁴⁻ anions. Since only the stability and loading of the cations are considered when they are covalently bonded to SBA-15, without burden of functionality incorporation, the selection of the cations becomes a more simple and flexible task. Then the functional moieties ([PdTSPP]⁴⁻) located in the anions can be maintained intact during the immobilization.

* Corresponding author. Fax: +86 21 62233424.

E-mail address: yliu@chem.ecnu.edu.cn (Y. Liu).



Scheme 1. Strategy for synthesizing SBA-15-supported Pd-porphyrin functionalized ILs: (a) post-synthesis, (b) one-pot sol-gel synthesis.

2. Experimental

2.1. Materials

Tetraethyl orthosilicate (TEOS), Pluronic P123 (poly(ethylene glycol)–poly(propylene glycol)–poly(ethylene glycol), average molecular mass 5800), 3-chloropropyltrimethoxysilane, N-methylimidazole were of commercial grade and used as received. The other reagents including PdCl₂, ethyl acrylate (AR), iodobenzene (AR), triethylamine (AR), and n-dodecane, etc. were purchased from Alfa Aesar.

2.2. Synthesis

2.2.1. Post-synthesis

2.2.1.1. Chloropropyl-grafted SBA-15 (Post-CP-SBA-15). SBA-15 was synthesized following the procedures reported by Zhao et al. [29].

5.6 g SBA-15 (calcined at 550 °C for 4 h) and 4.5 g 3-chloropropyltrimethoxysilane were mixed in 150 mL toluene and stirred vigorously for 1 h at room temperature. The obtained mixture after adding 0.65 g deionized water and 0.34 g toluene-p-sulfonic acid was stirred at 120 °C for 8 h. The obtained solid was washed with toluene, ethanol, and diethyl ether before dryness in oven at 90 °C, which was referred to as Post-CP-SBA-15.

2.2.1.2. Pd-porphyrin functionalized IL-modified SBA-15 (Post-PdTSPP-PMIM-SBA-15). 2.5 g Post-CP-SBA-15 and 0.3 g N-methylimidazole were mixed in 80 mL toluene. After refluxing for 15 h under vigorous stirring, the obtained solid was washed by ethanol and then dried in vacuo to give Post-PMIM-SBA-15.

To 600 mg Post-PMIM-SBA-15 was added 200 mg (meso-tetra-(p-sulfonatophenyl)-porphyrinato)palladium sodium ([PdTSPP]Na₄) [32] and 15 mL deionized water. The mixture was stirred

at room temperature for 8 h. The obtained brick-red solid was washed with water, ethanol, CH₃CN, Et₃N, and PhI, respectively, until the Soret band of [PdTSPP]Na₄ at 414 nm could not be observed in the final filtrate, which was detected by the UV–visible (UV–vis.) spectroscopy.

2.2.1.3. [PdTSPP]Na₄-modified SBA-15 ([PdTSPP]Na₄-SBA-15). For comparison [PdTSPP]Na₄-modified SBA-15 was prepared through wet impregnation method as follows. 300 mg SBA-15 was mixed with 43 mg [PdTSPP]Na₄ and 5 mL methanol. The mixture was stirred at room temperature for 1 h. However, when the obtained brick-red solid after filtration was washed with water and ethanol, its color changed to pale-yellow and the red filtrate was obtained, due to the loss of [PdTSPP]Na₄ out of SBA-15 surface. Hence, the brick-red solid after vacuum drying was directly used as the sample of [PdTSPP]Na₄-SBA-15 without further treatment. The inductive coupled plasma (ICP) analysis of Pd in [PdTSPP]Na₄-SBA-15 was 1.01 wt%. UV–vis. (solid disc, nm): 405 (Soret band, s), and Q bands (524 (s), 557(w), and 610 (w) nm), which are very similar to the characteristic absorbances of Post-PdTSPP-PMIM-SBA-15 (Fig. 3(a)).

2.2.2. One-pot-synthesis

2.2.2.1. Chloropropyl-grafted SBA-15 (One-pot-CP-SBA-15). Chloropropyl-grafted SBA-15 was synthesized following the procedures reported by Bordoloi et al. [33]. 4 g Pluronic P123 was added into 30 mL deionized water under vigorous stirring for 3 h, and then 120 g of 2.0 M HCl solution was added. The resultant mixture was stirred at 25 °C for 10 min, in which 8.50 g TEOS (40.7 mmol) and 0.81 g (4.07 mmol) 3-chloropropyltrimethoxysilane were subsequently introduced. The mixture was stirred vigorously at 35 °C for 24 h, and aged for another 24 h at 80 °C without stirring. The solid product was obtained after filtration, and then washed in HCl

(2.0 M)-ethanol solution under stirring for 3 h at 50 °C to remove the organic templates. The as-synthesized product was dried at 100 °C for 2 h to yield chloropropyl-grafted SBA-15 (referred to as One-pot-CP-SBA-15).

It was found that more ratio of 3-chloropropyltrimethoxysilane in TEOS led to unsuccessful preparation of typical mesoporous SBA-15.

2.2.2.2. Pd-porphyrin functionalized IL-modified SBA-15 (One-pot-PdTSPP-PMIM-SBA-15). Upon quaternizing One-pot-CP-SBA-15 by N-methyl imidazole and then ion-exchanging with [PdTSPP]Na₄, One-pot-PdTSPP-PMIM-SBA-15 was obtained following the similar procedures as described in the part for synthesizing Post-PdTSPP-PMIM-SBA-15.

2.3. Characterization

Fourier transform infrared (FT-IR) spectra were recorded on a Nicolet NEXUS 670 spectrometer. Elemental analyses for CHN were obtained by using an Elementar Vario EL III instrument; while Pd amount in the sample was quantified using ICP analysis on an IRIS Intrepid II XSP instrument (Thermo Electron Corporation). Powder X-ray diffraction (PXRD) patterns were collected on a Bruker AXS D8 ADVANCE with Cu K α radiation. Transmission electron microscopy (TEM) measurement was carried out on a JEM-2100 instrument (JEOL Ltd., resolution 5 nm). The samples were loaded on gold slices after sono-irradiation in acetone for TEM characterization. The UV-visible spectra were recorded on a SHIMADZU-UV 2550 spectrophotometer with resolution of ca. 1 nm. GC analyses were performed on a SHIMADZU-2014A chromatography equipped with Rtx-Wax capillary column (30 m \times 0.25 mm \times 0.25 μ m). The column temperature was programmed from 60 to 240 °C at a ramp of 10 °C/min with a hold time of 3 min at the initial temperature and 10 min at the final temperature. The injector temperature was 250 °C. The detector temperature was 250 °C. GC-MS analyses were recorded on an Agilent 6890 instrument equipped with Agilent 5973 mass selective detector. The same GC analysis conditions as mentioned above were applied to GC-MS analyses.

The pore diameter, pore volume, and surface area of the samples were obtained from N₂ sorption isotherm at 77 K using an Autosorb Quancachrome 02108-KR-1 instrument.

2.4. Catalytic activity test

Iodobenzene (2.5 mmol), ethyl acrylate (3.75 mmol), triethylamine (Et₃N, 3.75 mmol), and SBA-15-supported Pd-catalyst were mixed and sealed in the glass vial under vigorous stirring at appointed conditions on an Advantage Series TM 2410 Personal Screening Synthesizer (Argonaut Technologies Inc.). Upon completion, the reaction mixture was cooled to room temperature to yield a slurry solid which was extracted with diethyl ether (4 \times 2 mL). The ether fractions were combined, and then analyzed by GC to determine the conversions (n-dodecane as internal standard) and the selectivities (normalization method). The left solid containing the catalyst and the formed salt of Et₃N-HI was then used without further treatment for the next run.

3. Results and discussion

3.1. Characterization of the catalysts

According to the strategy in Scheme 1, the imidazolium-based IL grafted mesoporous silica, PMIM-SBA-15, was prepared through anchoring chloropropyl group to the framework of SBA-15 and then quaternizing N-methylimidazole. The subsequent ion-exchange with [PdTSPP]Na₄ in water afforded the SBA-15 supported

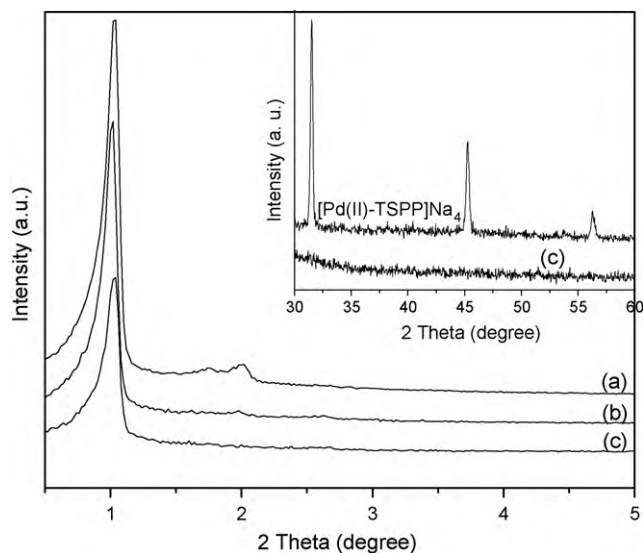


Fig. 1. PXRD patterns of (a) SBA-15, (b) Post-CP-SBA-15, and (c) Post-PdTSPP-PMIM-SBA-15.

Pd-porphyrin functionalized IL of PdTSPP-PMIM-SBA-15, which was thoroughly washed to remove the physically absorbed [PdTSPP]Na₄. The formation of highly water-soluble salt of NaCl is the driving force for such ion-exchange reaction. Based on such synthesis route, the covalently and stoichiometrically bonded 1-propyl-3-methylimidazolium cation without burden of the complicated catalytic site can guarantee the robustness of itself on SBA-15; Pd-porphyrin catalytic moiety located in the anion then can be maintained intactly, tightly, and stoichiometrically via the subsequent electrostatic interaction.

Firstly, the post-synthesized samples (Post-CP-SBA-15, and Post-PdTSPP-PMIM-SBA-15) were characterized by means of different techniques, including PXRD, FT-IR, UV-visible, ICP, N₂ sorption analysis, and TEM.

PXRD patterns in Fig. 1(b) show that Post-CP-SBA-15 exhibits an intensive reflection at $2\theta = 1.01^\circ$, which is characteristic of a two-dimensional hexagonal structure (*p6mm*) for typical SBA-15 silica (Fig. 1(a)). It is found that when grafting chloropropyl group in SBA-15 framework (1 0 0) reflection intensity decreases slightly, whereas (1 1 0) and (2 0 0) reflections are rarely observed (Fig. 1(c), CP-SBA-15-II). Upon quaternization by N-methyl imidazole and subsequent ion-exchange with [PdTSPP]Na₄, the obtained sample of Post-PdTSPP-PMIM-SBA-15 (Fig. 1(c)) exhibits the similar reflection at $2\theta = 1.03^\circ$ but with dramatic decrease of reflection intensity, due to the decrease of long-range order after modification. The slight shift of the characteristic reflection to higher degree is observed in Post-PdTSPP-PMIM-SBA-15, which corresponds to the decrease in d_{100} spacing from 8.65 to 8.49 nm as a cause of incorporation of organic functional group in host SBA-15 (Table 1) [31]. In the wide-angle region of PXRD (inset: $2\theta = 30\text{--}60^\circ$, Fig. 1(c)), the absence of [PdTSPP]Na₄ reflections suggests the high dispersion of [PdTSPP]⁴⁻ ions in the channels of SBA-15.

The sample of Post-PdTSPP-PMIM-SBA-15 was further characterized by FT-IR and UV-visible spectra. Upon functionalization, the typical IR vibration for silanol groups is observed at 3740 cm⁻¹, due to the exposure of hydroxyl derived from the partial collapse of host SBA-15 framework. This result is consistent to the decreased reflection intensity in XRD pattern for Post-PdTSPP-PMIM-SBA-15 due to the decrease of long-range order. The appearance of vibration peaks of C-H bonds (2800–3200 cm⁻¹), C=C bonds (\sim 1570 cm⁻¹), C=N bonds (\sim 1460 cm⁻¹) (Fig. 2) indicates the presence of 1-propyl-3-methylimidazolium group and porphyrino ring structure.

Table 1
Physicochemical properties of the post-synthesized samples^a.

Sample	PXRD d_{100} (nm)	N ₂ sorption isotherms			Elemental analysis	
		S_{BET} (m ² /g)	D_{BJH} (nm)	V_t (cm ³ /g)	Pd (wt %)	N (wt %)
Post-CP-SBA-15	8.65	509	4.19	0.52	–	–
Post-PdTSP-PMIM-SBA-15	8.49	220	4.76	0.27	1.37	2.98

^a S_{BET} , BET specific surface area; D_{BJH} , pore diameter calculated using BJH method; V_t , total pore volume; Pd amount was based on ICP-AES analysis; N amount was based on CHN-elemental analysis.

The UV–visible spectra of Post-PdTSP-PMIM-SBA-15 (solid disc) in Fig. 3(a) show the typical Sore (405 nm) and Q bands (524, 557, and 607 nm), which are similar to the characteristic absorbances of [PdTSPP]Na₄ dissolved in water (Fig. 3(b)). However, the absorbance intensity of Q bands of Post-PdTSP-PMIM-SBA-15 increases dramatically, implying the more active $\alpha_{2\mu}(\pi) \rightarrow e_g(\pi^*)$ transition [34,35], probably due to the changed $\pi-\pi^*$ interaction derived from the isolated [PdTSPP]⁴⁻ sites by SBA-15 skeleton.

N₂ adsorption–desorption isotherms for Post-CP-SBA-15 and resultant Post-PdTSP-PMIM-SBA-15 were given in Fig. 4. Table 1 summarized the results of N₂ sorption analysis, PXRD, and elemental analysis for Pd and N. The isotherms feature hysteresis loops with clear adsorption and desorption branches in the P/P_0 range of 0.4–0.7, indicating a narrow mesopore size distribution (Fig. 4(b)). After

capture of Pd-porphyrin functionalized IL, the total surface area (S_{BET}) and pore volume (V_t) decrease from 509 to 220 m²/g and from 0.52 to 0.27 cm³/g, respectively, along with a slight increase of the average pore size (D_{BJH}) from 4.19 to 4.76 nm due to the collapse of the partial mesopores. These results indicate that the void pores of Post-CP-SBA-15 have been occupied by Pd-porphyrin functionalized ILs.

Molar ratio 16 of N/Pd (Table 1) in sample Post-PdTSP-PMIM-SBA-15 also reveals that each [PdTSPP]⁴⁻ anion is counteracted by four imidazolium cations stoichiometrically with additional imidazolium chlorides distributed sparsely in the channel of host SBA-15.

The TEM images provide a direct visualization for the samples of Post-CP-SBA-15 and Post-PdTSP-PMIM-SBA-15. Fig. 5(a) clearly shows uniform and long-range ordered hexagonal channels of Post-CP-SBA-15 which are open for guest molecules to enter. Upon quaternization by N-methylimidazole and capture of [PdTSPP]⁴⁻

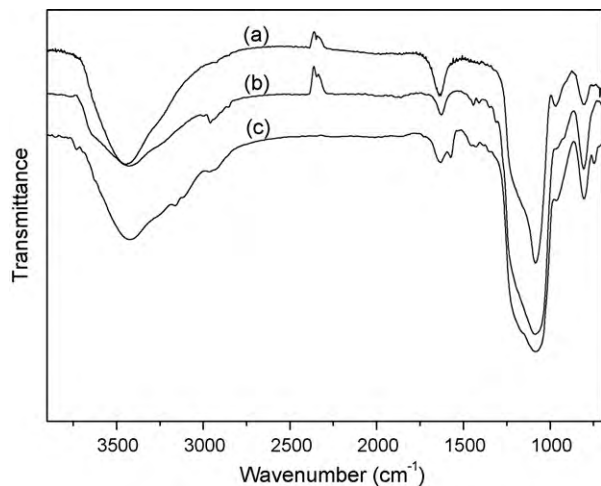


Fig. 2. FT-IR spectra of (a) SBA-15, (b) Post-CP-SBA-15, and (c) Post-PdTSP-PMIM-SBA-15.

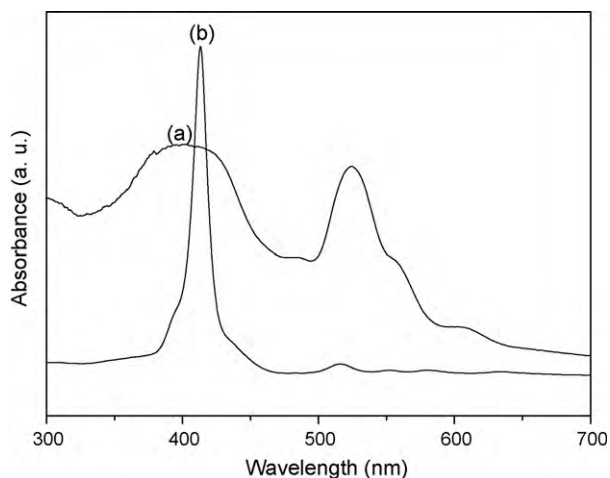


Fig. 3. UV–visible spectra of (a) Post-PdTSP-PMIM-SBA-15 (solid disc) and (b) [PdTSPP]Na₄ (in water).

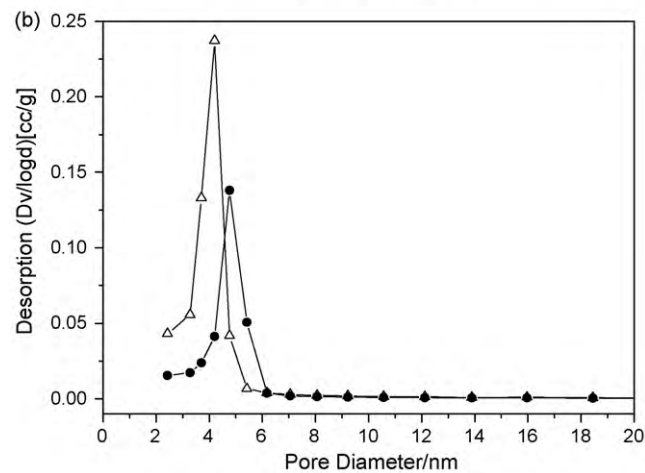
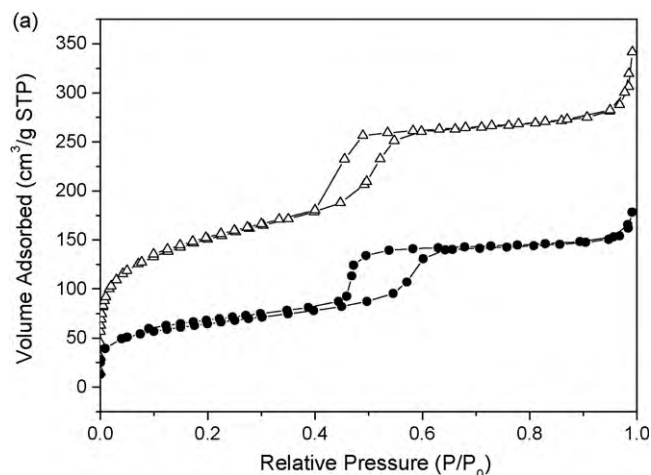


Fig. 4. (a) N₂ sorption isotherms of Post-CP-SBA-15 (Δ), and Post-PdTSP-PMIM-SBA-15 (\bullet); (b) Pore size distribution of Post-CP-SBA-15 (Δ), and Post-PdTSP-PMIM-SBA-15 (\bullet) calculated from the desorption branch of the isotherms using the BJH algorithm.

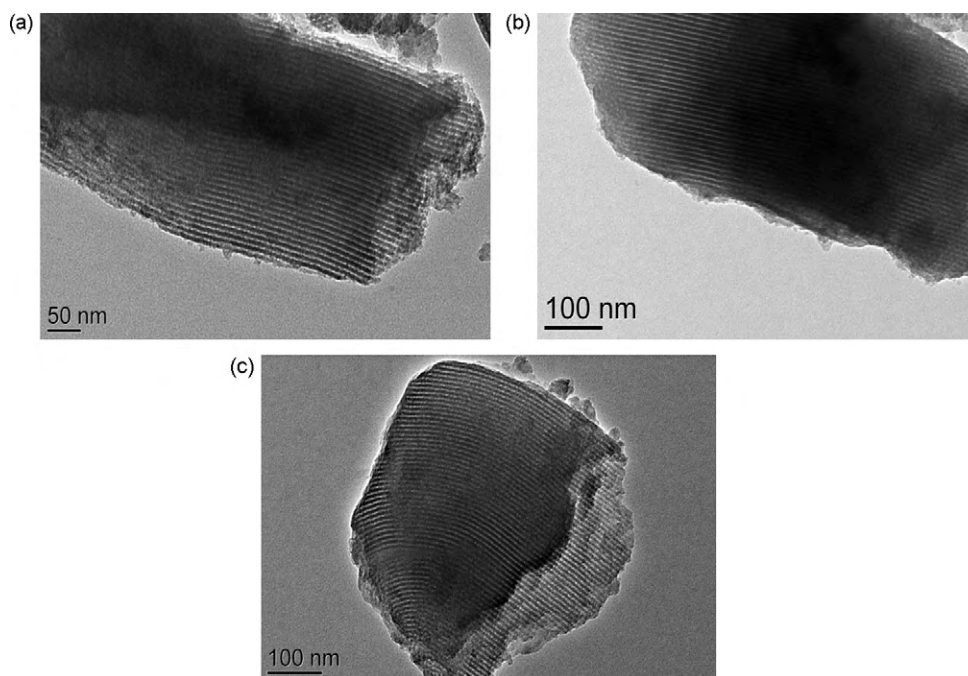


Fig. 5. TEM images of (a) Post-CP-SBA-15, (b) Post-PdTSP-PMIM-SBA-15, and (c) used Post-PdTSP-PMIM-SBA-15 after 9 runs.

anions, the typical mesophase maintains well without observable difference. Moreover, the absence of aggregated Pd nanoparticles indicates the high dispersion of $[\text{PdTSPP}]^{4-}$ ions in the channels of host SBA-15. The TEM observations are consistent to the PXRD and N_2 sorption isotherms results.

The characterizations of one-pot-synthesized materials (One-pot-CP-SBA-15, and One-pot-PdTSP-PMIM-SBA, see Figs. S1–S4 and Table S1 in Supplementary Information) reveal that SBA-15 mesoporous framework can be retained but with dramatic decrease of long-range order (Fig. S1(c) and Fig. S4(b)). When using one-pot synthesis method without calcining the materials at 550 °C, the relatively frail framework of SBA-15 could be destructed badly during the further modification or solvent treatment.

3.2. Catalytic performance

Post-PdTSP-PMIM-SBA-15 was selected to catalyze the Heck reaction of iodobenzene with ethyl acrylate as a model reaction,

Table 2

The Heck reaction of iodobenzene with ethyl acrylate catalyzed by Post-PdTSP-PMIM-SBA-15^a.

Entry	Catalyst	Yield (%) ^b
1	$[\text{PdTSPP}]\text{Na}_4$ (fresh)	91
2	PdTSP-PMIM-SBA-15-II (fresh)	100
3	PdTSP-PMIM-SBA-15-II (2nd run)	86
4	PdTSP-PMIM-SBA-15-II (3rd run)	72
5 ^c	PdTSP-PMIM-SBA-15-II (4th run)	88
6	PdTSP-PMIM-SBA-15-II (5th run)	91
7	PdTSP-PMIM-SBA-15-II (6th run)	85
8	PdTSP-PMIM-SBA-15-II (7th run)	85
9	PdTSP-PMIM-SBA-15-II (8th run)	84
10	PdTSP-PMIM-SBA-15-II (9th run)	73
11	$[\text{PdTSPP}]\text{Na}_4$ -SBA-15 (fresh)	79
12	$[\text{PdTSPP}]\text{Na}_4$ -SBA-15 (2nd run)	76
13	$[\text{PdTSPP}]\text{Na}_4$ -SBA-15 (3rd run)	6

^a Pd concentration 0.1 mol%, iodobenzene 0.5 mmol, Et_3N 1.0 mmol, ethyl acrylate 1.0 mmol, temperature 130 °C, time 3 h.

^b GC yields to *trans*-ethyl cinnamate.

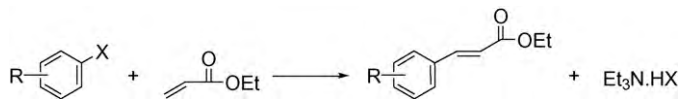
^c The used Post-PdTSP-PMIM-SBA-15 after the 3rd run was washed with CH_3CN and EtOH before next run.

due to high loading of Pd-catalyst (1.37 wt%) and well-retained SBA-15 structure (Table 2). The homogeneous catalyst of $[\text{PdTSPP}]\text{Na}_4$ was used as comparison. Since the reaction was carried out under solvent-free condition, the liquid organic amine of Et_3N was preferred as the base. Under mild conditions, 91% yield of *trans*-ethyl cinnamate was obtained in aerial atmosphere when homogeneous catalyst $[\text{PdTSPP}]\text{Na}_4$ was applied (Entry 1). Based on the same concentration benchmark, Post-PdTSP-PMIM-SBA-15 exhibited better activity (Entry 2), probably due to the individual isolation of $[\text{PdTSPP}]^{4-}$ catalytic sites in the channels of SBA-15, which blocked the aggregation of $[\text{PdTSPP}]^{4-}$ itself usually occurring in homogeneous processes [36]. Upon completion, the reaction mixture was extracted by ethyl ether. The left solid could be reused directly. However, after 3 runs, the conversion of iodobenzene decreased to 72% (Entry 4). The ICP-AES analysis indicated that the leaching of Pd in the combined organic phase after 3 runs was beyond the limit of detection ($<0.1 \mu\text{g/g}$). The UV-visible spectra also indicated that the loss of $[\text{PdTSPP}]^{4-}$ in the liquid phase was non-detectable. These results ruled out any involvement of palladium species that leached out of Post-PdTSP-PMIM-SBA-15 catalyst into the liquid phase (which guaranteed the observed catalysis was truly heterogeneous in nature). The UV-visible spectra (Fig. S5(b) in Supplementary Information) showed that the used Post-PdTSP-PMIM-SBA-15 was as intact as the fresh one in term of $[\text{PdTSPP}]^{4-}$ character. However, in FT-IR spectra (Fig. S6(b) in Supplementary Information), a strong peak at 1733 cm^{-1} ascribed to C=O vibration was observed, which revealed that the surface of Post-PdTSP-PMIM-SBA-15 was covered by the adsorbed *trans*-ethyl cinnamate, leading to inaccessibility of the substrate to the catalytic site and then the dropped activity. Hence, the left solid after the 3rd run (Entry 4) was washed with CH_3CN and EtOH thoroughly before continuous uses. Consequently, the activity of the resultant brick-red catalyst was almost recovered as shown in Entries 5–9 (Table 2). The TEM image in Fig. 5(c) also indicated that the used Post-PdTSP-PMIM-SBA-15 after 9 runs retained as intact as the fresh one in terms of SBA-15 mesoporous structure and $[\text{PdTSPP}]^{4-}$ dispersion.

In contrast, when $[\text{PdTSPP}]\text{Na}_4$ -SBA-15 was used as the catalyst (Entries 11–13 of Table 2), the activity lost rapidly during recycling.

Table 3

Heck reaction of aryl halides with ethyl acrylate catalyzed by Post-PdTSPP-PMIM-SBA-15^a



Entry	R	X	Yield (%) ^b
1	<i>p</i> -CH ₃	I	100
2	<i>m</i> -CH ₃	I	82
3	<i>p</i> -OCH ₃	I	100
4	<i>m</i> -OCH ₃	I	93
5	<i>p</i> -NO ₂	I	100
6	<i>m</i> -NO ₂	I	100
7	<i>p</i> -CF ₃	I	100
8	<i>m</i> -CF ₃	I	100
9	H	Br	<5
10	<i>p</i> -NO ₂	Br	83
11	<i>p</i> -CF ₃	Br	92
12	<i>p</i> -CH ₃	Br	<5
13	<i>p</i> -OCH ₃	Br	<5

^a Cat 0.1 mol%, substrate 0.5 mmol, Et₃N 1.0 mmol, ethyl acrylate 2 mmol, temperature 140 °C, reaction time 4 h.

^b GC yields to *trans*-coupling products (the products were confirmed by GC-Mass).

After the 2nd run, the white solid and a distinct red solution were obtained, due to the leaching of [PdTSPP]Na₄ out of SBA-15 into the liquid phase. Resultantly, the left white solid exhibited no any activity in the 3rd run. The UV–visible spectra of which showed that [PdTSPP]Na₄ barely existed on SBA-15. These results indicated that, without the aid of imidazolium cations which were covalently bonded on SBA-15 surface, the capture of [PdTSPP]⁴⁻ anions on SBA-15 was unavailable.

The generality of Post-PdTSPP-PMIM-SBA-15 to a wide array of substrates with different steric and electronic effects was listed in Table 3. It was indicated that, due to the high reactivity of aryl iodides, the cross-coupling products were obtained in excellent yields without obvious discrimination of electronic effect. However, the steric effect was obvious when the electron-rich substituent (–OCH₃ or –CH₃) was involved (Entries 2 and 4). As for the aryl bromides with relatively low reactivity, the activated substrates with electron-withdrawing character, such as *p*-bromonitrobenzene and *p*-bromotrifluoromethylbenzene, coupled with ethyl acrylate in good yields (Entries 10 and 11). The deactivated substrates such as *p*-bromotoluene and *p*-bromoanisole coupled in poor yields under the same reaction conditions (Entries 12 and 13).

4. Conclusions

The Pd-porphyrin functionalized ionic liquid can be tightly locked in the channels of mesoporous SBA-15 through ion-pair electrostatic interaction between imidazolium-cationic and Pd-porphyrin-anionic moieties. It was found that the materials prepared through post-synthesis maintained better mesophase structure of SBA-15 than those prepared through one-pot sol–gel procedure. The catalysis investigation proved that the material of Post-PdTSPP-PMIM-SBA-15 was an efficient heterogeneous cata-

lyst towards the Heck reaction of aryl iodides/bromides and ethyl acrylate in absence of any organic ligand and organic solvent, which could be recovered and recycled 9 times without SBA-15 structural collapse, Pd species leaching, and obvious activity loss.

Acknowledgements

The research work was financially supported by the National Natural Science Foundation of China (No. 20673039), the Science & Technology Commission of Shanghai Municipality (No. 09JC1404800), the Ministry of Science & Technology of China for Croatian-Chinese Scientific and Technological Cooperation, and the Fundamental Research Funds for the Central Universities.

Appendix A. Supplementary data

Supplementary data associated with this article can be found, in the online version, at doi:10.1016/j.materresbull.2010.07.006.

References

- [1] S. Bräse, A. de Meijere, in: A. Meijere, F. Diederich (Eds.), 2nd edition, Metal-Catalyzed Cross-Coupling Reactions, vol. 1, Wiley-VCH, Weinheim, 2004, pp. 217–315.
- [2] W. Kleist, S.S. Pröckl, K. Köhler, Catal. Lett. 125 (2008) 197.
- [3] M. Tada, Y. Iwasawa, Coord. Chem. Rev. 251 (2007) 2702.
- [4] A. Corma, H. Garcia, Adv. Synth. Catal. 348 (2006) 1391.
- [5] K. Ding, Pure Appl. Chem. 78 (2006) 293.
- [6] A. Marinas, J.M. Marinas, M.A. Aramendia, F.J. Urbano, New Develop. Catal. Res. (2005) 85.
- [7] H.-U. Blaser, A. Indolese, A. Schnyder, H. Steiner, M. Studer, J. Mol. Catal. A: Chem. 173 (2001) 3.
- [8] Y. Liu, S. Wang, W. Liu, Q. Wan, H. Wu, G. Gao, Curr. Org. Chem. 13 (2009) 1322.
- [9] V. Polshettiwar, R.S. Varma, Acc. Chem. Res. 41 (2008) 629.
- [10] S. Liu, J. Xiao, J. Mol. Catal. A: Chem. 270 (2007) 1.
- [11] M. Smiglak, A. Metlen, R.D. Rogers, Acc. Chem. Res. 40 (2007) 1182.
- [12] R. Šebesta, I. Kmentová, Š. Toma, Green Chem. 10 (2008) 484.
- [13] T. Fukushima, T. Aida, Chem. Eur. J. 3 (2007) 5048.
- [14] D.E. Bergbreiter, J. Tian, C. Hongfa, Chem. Rev. 109 (2009) 530.
- [15] P.H. Toy, K.D. Janda, Acc. Chem. Res. 33 (2000) 546.
- [16] I.T. Horvath, Acc. Chem. Res. 31 (1998) 641.
- [17] L.P. Barthel-Rosa, J.A. Gladysz, Coord. Chem. Rev. 190–192 (1999) 587.
- [18] X. Ma, Y. Zhou, J. Zhang, A. Zhu, T. Jiang, B. Han, Green Chem. 10 (2008) 59.
- [19] J.-Y. Jung, A. Taher, H.-J. Kim, W.-S. Ahn, M.-J. Jin, Synlett (2009) 39.
- [20] M.S. Sarkar, H. Qiu, M.-J. Jin, J. Nanosci. Nanotechnol. 7 (2007) 3880.
- [21] A. Safavi, N. Maleki, N. Iranpoor, H. Firouzabadi, A.R. Banazadeh, R. Azadi, F. Sedaghati, Chem. Commun. (2008) 6155.
- [22] B. Karimi, D. Enders, Org. Lett. 8 (2006) 1237.
- [23] H. Hagiwara, Y. Sugawara, T. Hoshi, T. Suzuki, Chem. Commun. (2005) 2942.
- [24] H. Hagiwara, Y. Sugawara, K. Isobe, T. Hoshi, T. Suzuki, Org. Lett. 6 (2004) 2325.
- [25] L. Wang, Y. Zhang, C. Xie, Y. Wang, Synlett (2005) 1861.
- [26] K. Anderson, F.S. Cortinas, C. Hardacre, P.C. Marr, Inorg. Chem. Commun. 7 (2003) 73.
- [27] W. Miao, T.H. Chan, Acc. Chem. Res. 39 (2006) 897.
- [28] C.P. Mehnert, Chem. Eur. J. 11 (2005) 50.
- [29] D.Y. Zhao, J.L. Feng, Q.S. Huo, N. Melosh, G.H. Frederickson, B.F. Chmelka, G.D. Stucky, Science 279 (1998) 548.
- [30] C. Kresge, M. Leonowicz, W. Roth, C. Vartuliand, J. Beck, Nature 359 (1992) 710.
- [31] C. Yang, P. Liu, Y. Ho, C. Chiu, K. Chao, Chem. Mater. 15 (2003) 275.
- [32] Z. Dong, P.J. Scammells, J. Org. Chem. 72 (2007) 9881.
- [33] A. Bordoloi, S. Sahoo, F. Lefebvre, S.B. Halligudi, J. Catal. 259 (2008) 232.
- [34] J.D. Petke, G.M. Maggiora, in: M. Gouterman, P.M. Rentzepis, K.D. Straub (Eds.), ACS Symposium Series 321, 1985, 20–50.
- [35] E.C.A. Ojadi, H. Linschitz, M. Gouterman, R.I. Water, J.S. Lindsey, R.W. Wagner, P.R. Droupadi, W. Wang, J. Phys. Chem. 97 (1993) 13192.
- [36] X.Q. Yu, J.S. Huang, W.Y. Yu, C.M. Che, J. Am. Chem. Soc. 122 (2000) 5337.